

Bryn Mawr College

## Scholarship, Research, and Creative Work at Bryn Mawr College

---

Physics Faculty Research and Scholarship

Physics

---

Winter 1-6-2016

### Observations of the high vibrational levels of the B<sup>2</sup>B 1Σ<sup>+</sup> state of H<sub>2</sub>

Alexander M. Chartrand

*Bryn Mawr College*, [achartrand@brynmawr.edu](mailto:achartrand@brynmawr.edu)

W. Duan

R. C. Ekey

Elizabeth McCormack

*Bryn Mawr College*

Follow this and additional works at: [https://repository.brynmawr.edu/physics\\_pubs](https://repository.brynmawr.edu/physics_pubs)



Part of the [Atomic, Molecular and Optical Physics Commons](#)

[Let us know how access to this document benefits you.](#)

---

#### Citation

Chartrand, Alexander M.; Duan, W.; Ekey, R. C.; and McCormack, Elizabeth, "Observations of the high vibrational levels of the B<sup>2</sup>B 1Σ<sup>+</sup> state of H<sub>2</sub>" (2016). *Physics Faculty Research and Scholarship*. 101. [https://repository.brynmawr.edu/physics\\_pubs/101](https://repository.brynmawr.edu/physics_pubs/101)

This paper is posted at Scholarship, Research, and Creative Work at Bryn Mawr College. [https://repository.brynmawr.edu/physics\\_pubs/101](https://repository.brynmawr.edu/physics_pubs/101)

For more information, please contact [repository@brynmawr.edu](mailto:repository@brynmawr.edu).

## Observations of the high vibrational levels of the B''B'1Σu+ state of H2

A. M. Chartrand, W. Duan, R. C. Ekey, and E. F. McCormack

Citation: *The Journal of Chemical Physics* **144**, 014307 (2016); doi: 10.1063/1.4939079

View online: <http://dx.doi.org/10.1063/1.4939079>

View Table of Contents: <http://scitation.aip.org/content/aip/journal/jcp/144/1?ver=pdfcov>

Published by the [AIP Publishing](#)

---

### Articles you may be interested in

[Coherent superposition of M-states in a single rovibrational level of H2 by Stark-induced adiabatic Raman passage](#)

*J. Chem. Phys.* **140**, 074201 (2014); 10.1063/1.4865131

[\[1 + 1\] photodissociation of CS 2 + \(X̄ 2 Π g\) via the vibrationally mediated B' 2 Σ u + state: Multichannels exhibiting and mode specific dynamics](#)

*J. Chem. Phys.* **134**, 114309 (2011); 10.1063/1.3567071

[Spectral identification of diffuse resonances in H2 above the n = 2 dissociation limit](#)

*J. Chem. Phys.* **134**, 054309 (2011); 10.1063/1.3544300

[Observation of the 5 p Rydberg states of sulfur difluoride radical by resonance-enhanced multiphoton ionization spectroscopy](#)

*J. Chem. Phys.* **128**, 144306 (2008); 10.1063/1.2889382

[Heteronuclear rare-gas dimer bonding: Understanding the nature of the Rydberg states that dissociate to the highest energy level of the Xe \\* \(5d\) manifold](#)

*J. Chem. Phys.* **111**, 2985 (1999); 10.1063/1.479581

---



**NEW Special Topic Sections**

**NOW ONLINE**  
Lithium Niobate Properties and Applications:  
Reviews of Emerging Trends

**AIP** | Applied Physics  
Reviews

# Observations of the high vibrational levels of the $B''\bar{B}^1\Sigma_u^+$ state of $H_2$

A. M. Chartrand,<sup>1,a)</sup> W. Duan,<sup>2</sup> R. C. Ekey,<sup>3</sup> and E. F. McCormack<sup>1</sup>

<sup>1</sup>Department of Physics, Bryn Mawr College, Bryn Mawr, Pennsylvania 19010, USA

<sup>2</sup>Department of Electrical and Computer Engineering, University of Iowa, Iowa City, Iowa 52242, USA

<sup>3</sup>Physics and Astronomy Department, University of Mount Union, Alliance, Ohio 44601, USA

(Received 2 November 2015; accepted 15 December 2015; published online 6 January 2016)

Double-resonance laser spectroscopy via the  $EF^1\Sigma_g^+, v' = 6, J' = 0-2$  state was used to probe the high vibrational levels of the  $B''\bar{B}^1\Sigma_u^+$  state of molecular hydrogen. Resonantly enhanced multiphoton ionization spectra were recorded by detecting ion production as a function of energy using a time of flight mass spectrometer. New measurements of energies for the  $v = 51-66$  levels for the  $B''\bar{B}$  state of  $H_2$  are reported, which, taken with previous results, span the  $v = 46-69$  vibrational levels. Results for energy levels are compared to theoretical close-coupled calculations [L. Wolniewicz, T. Orlikowski, and G. Staszewska, *J. Mol. Spectrosc.* **238**, 118–126 (2006)]. The average difference between the 84 measured energies and calculated energies is  $-3.8\text{ cm}^{-1}$  with a standard deviation of  $5.3\text{ cm}^{-1}$ . This level of agreement showcases the success of the theoretical calculations in accounting for the strong rovibronic mixing of the  $^1\Sigma_u^+$  and  $^1\Pi_u^+$  states. Due to the ion-pair character of the outer well, the observed energies of the vibrational levels below the third dissociation limit smoothly connect with previously observed energies of ion-pair states above this limit. The results provide an opportunity for testing a heavy Rydberg multi-channel quantum defect analysis of the high vibrational states below the third dissociation limit. © 2016 AIP Publishing LLC. [<http://dx.doi.org/10.1063/1.4939079>]

## I. INTRODUCTION

The  $B''\bar{B}^1\Sigma_u^+$  double-well state is the third in a series of *ungerade* sigma states of the hydrogen molecule,  $H_2$ . As shown in Fig. 1, at small internuclear distances, the  $B''$  well corresponds to the  $(1s\sigma, 4p\sigma)$  molecular state. The outer  $\bar{B}$  well is formed by an avoided crossing with the  $(2s\sigma, 2p\sigma)$  doubly excited state at an internuclear distance of around  $5.7 a_0$  and an avoided crossing with the ion-pair  $H^+H^-$  potential around  $12 a_0$ .<sup>1,3-6</sup> At  $36 a_0$ , the potential energy curve experiences another avoided crossing and converges to the  $n = 3$  dissociation threshold. This work focuses on the high vibrational levels, which lie above the  $n = 2$  dissociation threshold and the ionization potential of the molecule, as well as above the double-well barrier. The outer well extends over a long range of internuclear distances such that its highest vibrational levels have turning points in the range of  $25-30 a_0$ . The above-barrier rovibrational levels of this state provide an excellent system to probe the accuracy of long-range, high energy calculations of  $H_2$ .

Previous studies by our group and others have reported energies for the  $v = 24-45$  states ( $v = 17-35$  of the outer well) which lie below the double-well barrier.<sup>8,9</sup> More recently, we have reported energy values for the  $v = 46-50$  states<sup>8</sup> and the  $v = 67-69$  states,<sup>10</sup> all of which lie above the barrier. These results were obtained by using resonantly enhanced multiphoton ionization spectroscopy. In a vacuum ultraviolet (VUV) spectroscopy study, Glass-Maujean *et al.*<sup>6</sup> measured energies for the above-barrier  $v = 46-63$  vibrational levels with a precision of  $\sim 8\text{ cm}^{-1}$ . The most recent theoretical study of the  $B''\bar{B}^1\Sigma_u^+$  state is that of Wolniewicz, Orlikowski, and

Staszewska,<sup>11</sup> where they calculate term energies and mixing matrix elements of the six lowest  $^1\Sigma_u$  states, shown in Fig. 1 and the four lowest  $^1\Pi_u$  states, shown in Fig. 2, by taking into account nonadiabatic corrections and electronic mixing of the  $^1\Sigma_u$  and  $^1\Pi_u$  states. For the  $B''\bar{B}^1\Sigma_u^+$  state in particular, they report mixing coefficients for each rovibrational level.

Here, we report measured term energies obtained by using resonantly enhanced, multiphoton ionization and time-of-flight mass spectroscopy. The results include values for the  $v = 46-66$  rovibrational levels of the  $B''\bar{B}^1\Sigma_u^+$  state, with energy uncertainties averaging  $\sim 0.5\text{ cm}^{-1}$ . Based on these measurements, we have made many new and some revised assignments. We also confirm several examples of unusual rotational structure predicted by the calculations of Wolniewicz, Orlikowski, and Staszewska<sup>11</sup> and discuss the opportunity to model the high  $v$  states using a multi-channel quantum defect theory approach.<sup>12</sup>

## II. EXPERIMENT

Double resonance spectroscopy via the  $J' = 0-2$  rotational levels of the  $EF^1\Sigma_g^+, v' = 6$  state was used to probe the energy region between  $131\,100$  and  $133\,700\text{ cm}^{-1}$  above the  $X^1\Sigma_g^+, v'' = 0, J'' = 0$  ground state of  $H_2$ . Ionization spectra were obtained by monitoring the production of atomic hydrogen ions using a time of flight mass spectrometer. The experimental arrangement has been described in detail previously.<sup>13</sup> Two pulsed Nd:YAG-pumped dye lasers and a vacuum chamber housing a pulsed-valve molecular beam source and a time of flight mass spectrometer were used to obtain double-resonance ionization spectra. Pump light with a wavelength near  $193\text{ nm}$  is used to excite the  $EF^1\Sigma_g^+, v' = 6$ ,

<sup>a)</sup>achartrand@brynmawr.edu

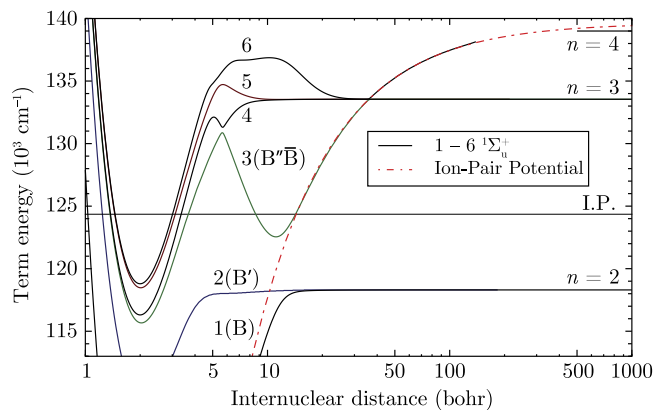


FIG. 1. *Ab initio* potential energy curves of the six lowest  $^1\Sigma_u$  states (Ref. 1) of  $\text{H}_2$  and the ion-pair  $\text{H}^+\text{H}^-$  potential (Ref. 2).

$J' = 0-2 \leftarrow X^1\Sigma_g^+, v'' = 0, J'' = 0-2$  two-photon transitions. This light was generated by sum-frequency mixing in a beta barium borate (BBO) crystal the fourth harmonic of Nd:YAG laser light at 266 nm with the output of a pumped dye laser operated at  $\sim 705$  nm. Probe laser output at 663–710 nm from the second dye laser was frequency doubled in a BBO and then used to excite single photon transitions from the  $EF^1\Sigma_g^+$  state to the states of interest as depicted in Fig. 3.

A collision-free beam of molecular hydrogen was produced by using a supersonic expansion of pure  $\text{H}_2$  from a solenoid-driven pulsed valve. Counter-propagating pump and probe light pulses crossed the molecular beam in an interaction region located between two electric field plates. The pump light pulses were typically on the order of 30  $\mu\text{J}$  and focused into the chamber with a 50-cm lens. Probe light pulses were focused into the chamber with a 30-cm lens to a spot size of  $\sim 100$   $\mu\text{m}$ . Ions generated by the two-colour process were accelerated into the time of flight mass spectrometer by a pulsed electric field of 125 V/cm applied across the plates. A time delay of 40 ns was introduced between the pump and probe laser pulses to distinguish ions produced by the pump beam alone and those produced by two-colour resonant excitation. Spectra are produced by scanning the frequency of the probe light while monitoring the production of  $\text{H}^+$  ions by using a boxcar integrator with a timed gate set to collect the

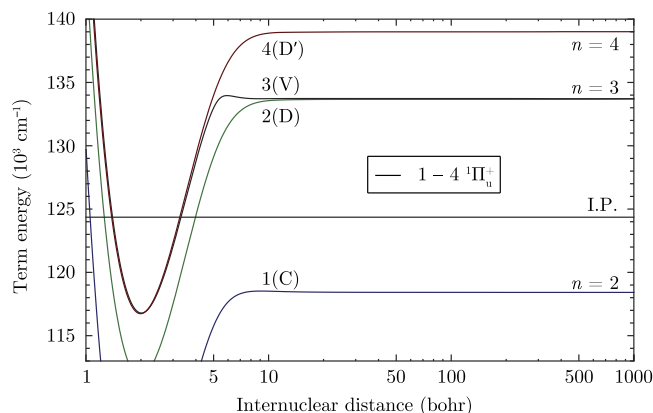


FIG. 2. *Ab initio* potential energy curves (Ref. 7) of the four lowest  $^1\Pi_u$  states of  $\text{H}_2$ .

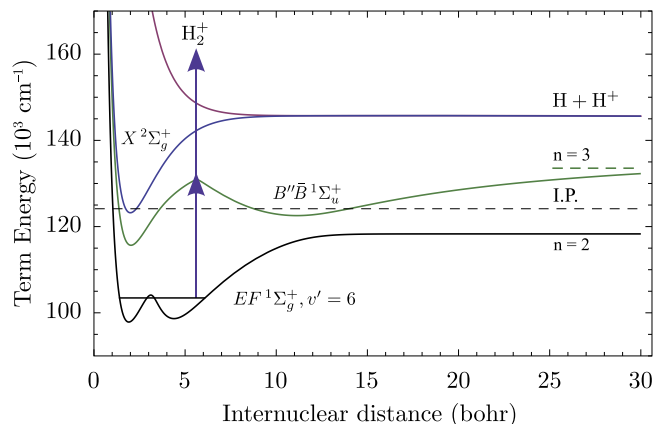


FIG. 3. Probe excitation scheme and generation of  $\text{H}^+$  ions.

ions. The optogalvanic effect in argon provides reference transitions at known energies and an etalon provides an independent measure of the linearity of the wavelength scans. Both are used to provide calibrated probe laser wavelengths. The energy uncertainties reported in Sec. III are standard deviations observed from data taken from multiple scans. They reflect the uncertainty associated with the calibration peaks, the statistical uncertainties of peak fits to the spectral features and remaining scan nonlinearities in the spectra. Reported total energies are referenced to the  $X^1\Sigma_g^+, v'' = 0, J'' = 0$  ground state by using the known  $EF^1\Sigma_g^+, v' = 6$  transition energies.<sup>14</sup>

### III. RESULTS AND DISCUSSION

Table I lists the observed term energies of the  $B''\bar{B}^1\Sigma_u^+$  state. The results for  $v = 67-69$  from Ref. 10 are included for completeness. The assignments listed were guided by the calculations of Wolniewicz, Orlikowski, and Staszewska.<sup>11</sup> In cases where states are strongly mixed, assignments are labeled by the dominant mixed-state characteristic. In addition, supplemental computations of rovibrational energies made in LEVEL 8.0<sup>15</sup> using previously published potential energy curves of other valence states<sup>17</sup> also guided assignments. Measured spectra are shown in Figs. 4 and 5, with labels of transitions to levels of the  $B''\bar{B}^1\Sigma_u^+$  state. Assignments to the  $4^1\Sigma_u^+$  state are also shown to aid the discussion. Details about the  $4^1\Sigma_u^+$  state and other unlabeled features corresponding to other known states in this energy region will be discussed in a future publication.

Figs. 6–8 are plots of measured and theoretically predicted term energies of the  $B''\bar{B}^1\Sigma_u^+$  state vs.  $J(J+1)$ . These plots highlight deviations from the linear dependence predicted by a simple rigid rotor model of the molecule. These deviations arise from couplings among the various rovibronic states. There are notable agreements and discrepancies.

Fig. 9 shows a histogram of the differences between our observed energies for levels of the  $B''\bar{B}^1\Sigma_u^+$  state and those of the theoretical calculations.<sup>11</sup> The histogram shows an average difference of  $-3.8$   $\text{cm}^{-1}$  and a standard deviation of  $5.3$   $\text{cm}^{-1}$ . As discussed in Ref. 11, this systematic shift

TABLE I.  $B''\bar{B}^1\Sigma_u^+$  state term energies in  $\text{cm}^{-1}$ .  $\Delta$  denotes the difference between current observed values and previous calculated values (Ref. 11). Uncertainties in the last digit are noted in parentheses.

$v$	$J$	Term energy	$\Delta$	$v$	$J$	Term energy	$\Delta$	$v$	$J$	Term energy	$\Delta$
46	0	131 187.6(4)	-6.5	54	0			62	0	132 953.5(3)	+0.0
	1	131 197.5(2)	-4.2		1		1		132 962.7(6)	-1.2	
	2	131 207.1(3)	-2.4		2		2		132 971.7(2)	-32	
	3	131 214.4(5)	-2.2		3		3				
	4	131 222.3(2)	-1.9		0	132 143.6(1)	-2.5		63	0	133 049.1(3)
47	0	131 246.3(6)	+2.5	1	132 147.5(3)	-3.7	1	133 055.2(4)	-2.8		
	1			2	132 148.7(2)	-2.0	2				
	2	131 295.3(2)	-5.0	3	132 157.3(7)	-13	3	133 111.3(3)	-7.3		
	3	131 340.0(6)	-4.0	55	0			64	0		
	4	131 360(1)	-3.1		1	132 260.2(3)	-2.2		1	133 151.1(5)	-1.8
48	0	131 356.6(2)	-2.2	2	132 264.9(2)	-2.4	2	133 163.0(1)	-1.5		
	1	131 359.3(7)	-2.1	3	132 270.2(5)	-1.5	3				
	2	131 365.7(3)	-3.3	56	0	132 369.7(1)	-2.2	65	0		
	3	131 391.7(2)	-7.5		1	132 371.7(2)	-2.2		1	133 244.5(4)	-2.9
	49	4	131 462.3(1)	-7.0	2	132 376.2(2)	-2.2	2	133 253.4(2)	-2.9	
0		131 493(1)	-1.5	3	132 384.0(3)	-2.0	3	133 295.7(2)	+18		
1		131 494.3(2)	-2.1	57	0			66	0	133 334.6(2)	-2.9
2		131 498.3(5)	-2.0		1		1		133 337.4(2)	-2.6	
50		3	131 504.5(6)	-3.0	2		2	133 343.5(3)	-2.9		
	4	131 522.2(1)	-5.1	3		3	133 360.4(2)	-0.0			
	58	0	131 632.7(2)	-5.1	0			67	0	133 425.7(4)	-2.9
		1	131 629.7(3)	-2.1	1	132 570.4(3)	-3.7		1	133 427.4(2)	
	51	2	131 633.0(1)	-2.1	2	132 574.7(7)	-4.5	2	133 433.0(4)	-3.0	
3		131 637.9(5)	-2.7	3	132 584.3(3)	-5.9	3	133 442.2(2)	-3.3		
4		131 647.0(2)	-2.3	59	0			68	0	133 514.0(3)	-3.0
0		131 755.6(1)	-5.5		1	132 654.6(4)	-4.7		1	133 515.0(2)	
52		1	131 757.8(2)	-2.5	2	132 655.9(2)	-6.6	2	133 518.8(2)	-3.4	
	2	131 761.4(2)	-3.9	3	132 662.4(3)	-10	3	133 526.6(2)			
	3	131 768.2(4)	-2.6	60	0	132 754.3(5)	-3.5	69	0	133 595.4(2)	
	4	131 776.1(1)	-2.1		1	132 743.7(8)	-5.6		1	133 596.3(2)	
	61	0	131 875(3)	-3.8	2	132 742.9(4)	-6.9	2	133 597.2(3)		
1		131 889.2(2)	+1.0	3	132 738.7(2)	-14	3	133 601.4(2)			
2		131 885.3(1)	-4.5	0	132 849.7(4)	-4.4					
62		1	131 895.8(2)	-2.0	1	132 891.1(6)	-4.9				
		2			2	132 909.0(5)	-22				
				3							

may be attributed to the limited number of electronic states included in the calculations as well as residual convergence errors in the Born-Oppenheimer potential of the  $B''\bar{B}^1\Sigma_u^+$  state.

Notably, Wolniewicz, Orlikowski, and Staszewska<sup>11</sup> predict several instances of what we are calling rotational inversions which are confirmed by our measurements. A rotational energy inversion is where a rotational series for a given vibrational state experiences a decrease in term energy with increasing rotational quantum number  $J$  due to electronic coupling with nearby states. The calculated and observed inversions are most easily seen in Figs. 6–8. The  $v = 60$  rovibrational levels are an extreme example of such an inversion. The perturber in this case is presumably the nearby  $4^1\Sigma_u^+$ ,  $v = 10$  state, which mixes with the  $v = 60$  state with coefficients ranging from 10%–18% for  $J = 0$ –3. In addition to the predicted inversions for  $v = 50$  and 60, we also observe a rotational inversion in the  $v = 52$  state; our measured value for the  $J = 1$  level is higher than the  $J = 2$  level. The confirmation of the predicted rotational inversions

is a testament to the success of the theoretical treatment in accounting for rovibronic mixing.

Exceptions are the three major outliers shown in Fig. 9, located in the histogram at  $-22$ ,  $-32$ , and  $+18 \text{ cm}^{-1}$ . We have assigned the observed energies of these outliers to  $v = 61$ ,  $J = 2$ ;  $v = 62$ ,  $J = 2$ ; and  $v = 65$ ,  $J = 3$ , respectively. In all three cases, Wolniewicz, Orlikowski, and Staszewska<sup>11</sup> predict significant mixing: in the first two cases with the  $V^1\Pi_u^+$ ,  $v = 9$  state and in the latter case with the  $4^1\Sigma_u^+$ ,  $v = 10$  state. The challenge of accurately predicting the mixing may account for the larger discrepancies between measured and calculated energies of these states.

In our previous work,<sup>8</sup> we assigned several spectral features that, in light of the calculations by Wolniewicz, Orlikowski, and Staszewska,<sup>11</sup> should be reassigned. First, as pointed out in Refs. 6 and 11, features that were assigned to the  $v = 48$  level of the  $B''\bar{B}^1\Sigma_u^+$  state should be reassigned to the  $D^1\Pi_u^+$ ,  $v = 12$  state. In addition, the measured energies attributed to the  $v = 47$  vibrational level in our previous work and that of Glass-Maujean *et al.*<sup>6</sup> should be reassigned to

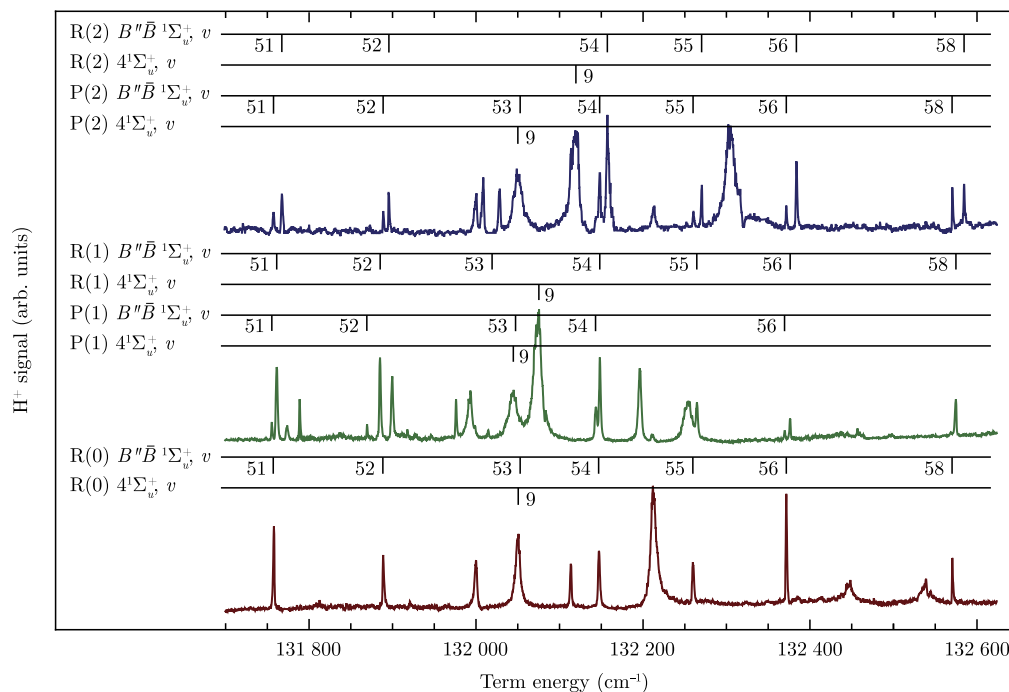


FIG. 4. Spectra of the  $B''\bar{B} \ ^1\Sigma_u^+$  spanning the  $v = 51$ – $58$  energy region. From bottom to top are the  $J' = 0$  (red),  $J' = 1$  (green), and  $J' = 2$  (blue) pump lines.

the  $v = 48$  level, in agreement with Wolniewicz, Orlikowski, and Staszewska.<sup>11</sup> Finally, our previously assigned  $v = 50$ ,  $J = 0$  level has been reassigned to a  $4 \ ^1\Sigma_u^+$  level, and a new assignment has been made for  $v = 50$ ,  $J = 0$  in good agreement with the theoretical prediction for this level. These updated assignments are reflected in Table I.

We note that in this work and that of Glass-Maujean *et al.*,<sup>6</sup> the  $v = 47$ ,  $J = 1$  level is unobserved. According to the theoretical predictions,<sup>11</sup> this state is highly mixed with the  $n = 2$  continuum of the  $B \ ^1\Sigma_u^+$  (16.4%) and  $B' \ ^1\Sigma_u^+$  (19.8%)

states, which would cause it to rapidly predissociate. The  $J = 0, 2$ , and  $3$  levels of the  $v = 47$  state, however, are not strongly mixed with the continuum ( $< 5\%$ ), and transitions to these levels are observed in our spectra.

In Table I, we do not report energies for levels of the  $v = 53$  and  $57$  vibrational states. The  $v = 53$  state is strongly mixed with several other states including the  $4$  and  $5 \ ^1\Sigma_u^+$  and  $D' \ ^1\Pi_u^+$  states. In the spectra shown in Fig. 4, the broad linewidth of the transition to the  $4 \ ^1\Sigma_u^+$ ,  $v = 9$  vibrational level obscures the energy region of the  $v = 53$  state such that we

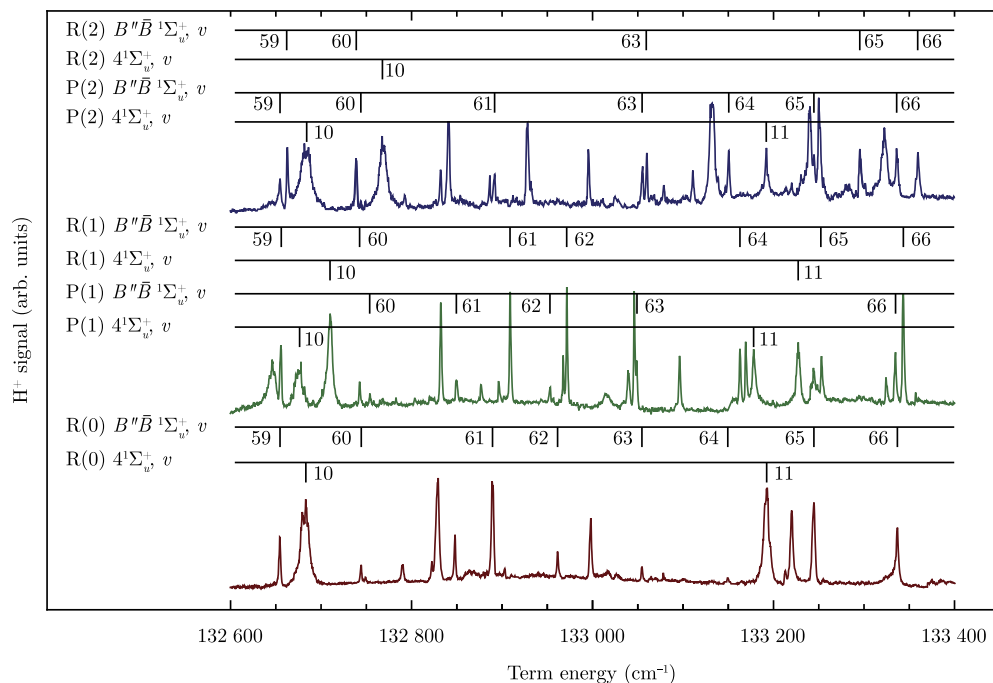


FIG. 5. Same as Fig. 4 spanning the  $v = 59$ – $66$  energy region.

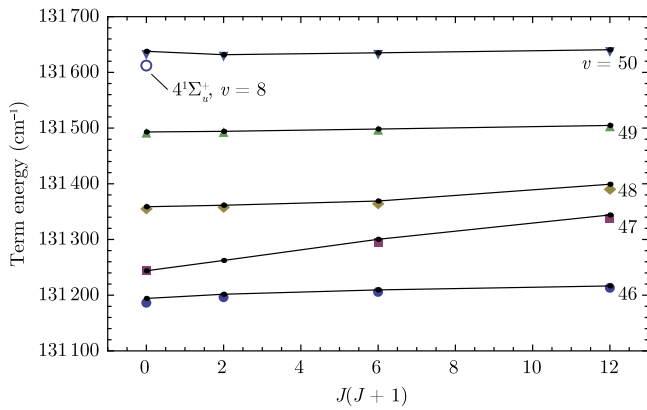


FIG. 6. Plots of term energy vs.  $J(J+1)$  for the  $v=46$ – $50$  energy region. Solid data points are  $B''\bar{B}^1\Sigma_u^+$  vibrational levels, whereas open symbols are other valence states. Connected black dots are theoretically calculated values from Ref. 11.

are unable to assign features to it. Instead, markers are placed at the theoretical values of the  $v=53$  rovibrational levels for reference.

The lack of observations of transitions to the  $v=57$  state may be explained by the Franck-Condon (FC) overlap with the  $EF^1\Sigma_g^+$ ,  $v'=6$  state. When plotting the Franck-Condon factor (FCF) output obtained by using LEVEL 8.0, as a function of the  $B''\bar{B}^1\Sigma_u^+$  vibrational quantum number, there is a minimum at  $v=57$ . There, the FCF is lower than the neighboring vibrational levels by a factor of between 10 and 100, depending on rotational level.

Finally, the connection between these high vibrational states and the *ungerade* ion-pair series is interesting to note. For the high vibrational levels of the  $B''\bar{B}^1\Sigma_u^+$  state below the third dissociation threshold, the outer turning points lie on the ion-pair potential curve, so we expect that these states possess ion-pair character. Above the third dissociation threshold, ion-pair states have been studied experimentally by our group<sup>13</sup> and theoretically using multi-channel quantum defect theory (MQDT) by Kirrander and Jungen.<sup>12</sup>

Fig. 10 shows a plot of the measured energy spacing of the  $B''\bar{B}^1\Sigma_u^+$  vibrational levels and ion-pair energy levels, defined as  $\Delta E = E_{v+1,n+1} - E_{v,n}$ , where  $v$  and  $n$  are the vibrational and energy quantum numbers, respectively. The ion-pair  $n$  values were assigned with the assistance of a MQDT model

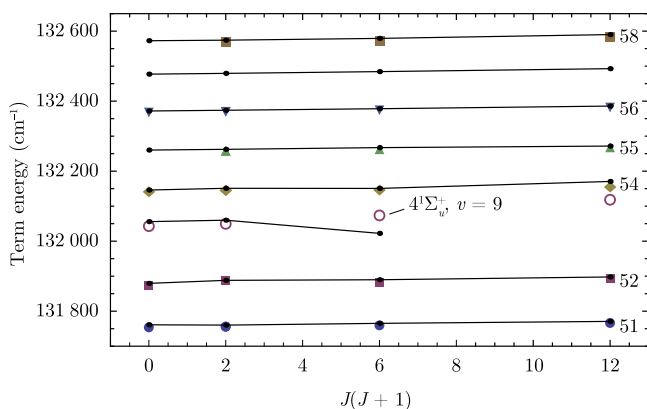


FIG. 7. Same as Fig. 6 for the  $v=51$ – $58$  energy region.

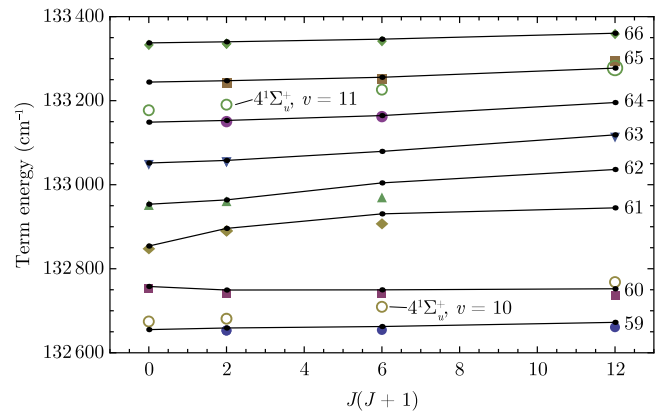


FIG. 8. Same as Fig. 6 for the  $v=59$ – $66$  energy region.

of the ion-pair states.<sup>16</sup> The dashed line in Fig. 10 represents the spacing one obtains from the ion-pair, heavy Rydberg formula,<sup>5,12,17</sup>

$$\frac{E_n}{hc} = D_{\text{H}^+\text{H}^-} - \frac{R_\infty(M/m_e)}{(n-\mu)^2}, \quad (1)$$

where  $D_{\text{H}^+\text{H}^-}$  is the dissociation limit of  $\text{H}^+ + \text{H}^-$ ,  $R_\infty$  is the infinite-mass Rydberg constant,  $\mu$  is the quantum defect,  $M$  is the reduced mass of the ion-pair configuration of  $\text{H}_2$ , and  $m_e$  is the electron mass.

A connection between the two sets of quantum numbers,  $n$  and  $v$ , has been established by Pan and Mies<sup>5,17</sup> to be

$$n \leftrightarrow v + J + 1 \quad (2)$$

by relating the number of nodes in a vibrational wavefunction to those of a Rydberg state wavefunction. As seen in Fig. 10, the spacing trend observed between high vibrational levels of the  $B''\bar{B}^1\Sigma_u^+$  state and ion-pair states decreases with increasing term energy, connecting smoothly through the dissociation threshold. At high energies, the heavy Rydberg model (Eq. (1)) accounts for the observed energy spacings well. Approaching the dissociation limit, the high  $v$  levels of the  $B''\bar{B}^1\Sigma_u^+$  state begin to deviate from the heavy Rydberg model, indicating that the strictly ion-pair configuration is beginning to break down.

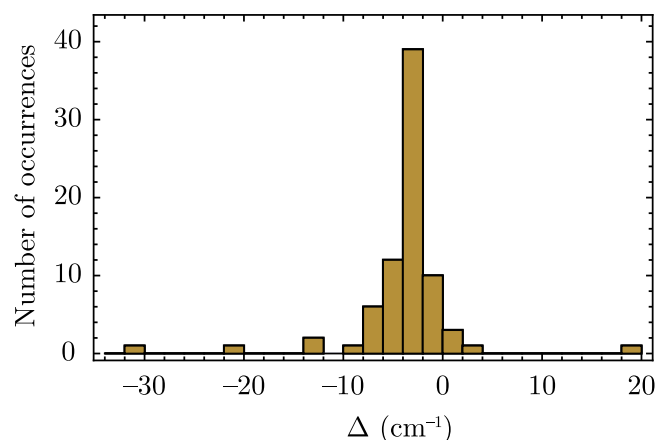


FIG. 9. Histogram of the discrepancy  $\Delta$  (current observations — previous calculations) from Table I. The average is  $-3.8 \text{ cm}^{-1}$  with a standard deviation of  $5.3 \text{ cm}^{-1}$ .

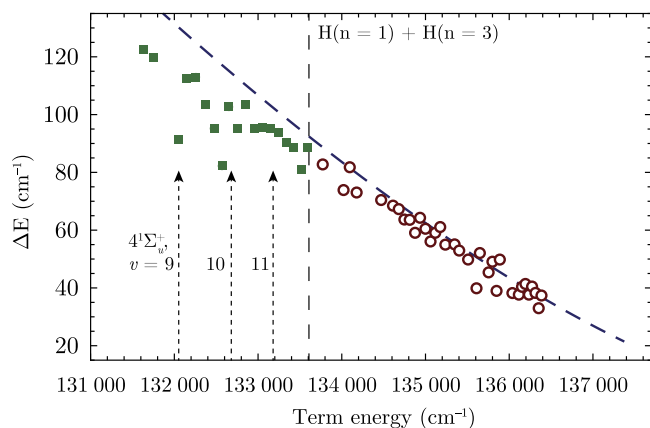


FIG. 10. Plot of observed energy spacing vs. observed term energy of  $B''\bar{B}^1\Sigma_u^+$ ,  $v = 51-68$ ,  $J = 0$  levels (solid green squares) and ion-pair energy levels (open red circles). The dashed blue line is the theoretical spacing obtained from the ion-pair Rydberg formula (Eq. (1)) with a quantum defect of zero. Unobserved  $B''\bar{B}^1\Sigma_u^+$  levels are included using the theoretical predictions with the systematic offset included.

In addition, the larger, periodic deviations can be explained by perturbations due to the  $4^1\Sigma_u^+$   $v = 9-11$  states.

#### IV. CONCLUSION

Double-resonance laser spectroscopy via the  $EF^1\Sigma_g^+$ ,  $v' = 6$ ,  $J'$  state was used to probe an energy region of  $2000\text{ cm}^{-1}$  containing the high-vibrational states of the  $B''\bar{B}^1\Sigma_u^+$  state below the third dissociation threshold and above the double-well barrier. Energies of the  $v = 46-69$  levels of the  $B''\bar{B}^1\Sigma_u^+$  of  $H_2$  are reported and, given the challenges with calculating highly mixed, long-range, high vibrational levels of this light molecule, compare favorably to the theoretical calculations of Wolniewicz, Orlikowski, and Staszewska.<sup>11</sup> We also compare the observed high vibrational series to the above-threshold observed ion-pair series of states. In principle, it should be possible to extend the MQDT treatment of Kirrander and Jungen<sup>12</sup> through the third dissociation threshold to calculate energies for the high- $v$   $B''\bar{B}^1\Sigma_u^+$  states. Such a calculation would provide an opportunity to compare the results of the MQDT approach to those of the close-coupled approach for these long-range, high energy states of  $H_2$ .

#### ACKNOWLEDGMENTS

We would like to thank KyungIn Kim and Zhongying Yan for their assistance with this project.

- <sup>1</sup>G. Staszewska and L. Wolniewicz, "Adiabatic energies of excited  $^1\Sigma_u$  states of the hydrogen molecule," *J. Mol. Spectrosc.* **212**, 208 (2002).
- <sup>2</sup>A. Kirrander, "Communication: Heavy Rydberg states: The  $H^+H^-$  system," *J. Chem. Phys.* **133**, 121103 (2010).
- <sup>3</sup>We note that the inner wall of the outer well can also be described due to the one-electron correlation of the  $(1s\sigma, 4f\sigma)$  state with the  $n = 2$  dissociation limit. See footnote e of Table II of Ref. 4.
- <sup>4</sup>R. S. Mulliken, "The Rydberg states of molecules. VI. Potential curves and dissociation behavior of (Rydberg and other) diatomic states," *J. Am. Chem. Soc.* **88**, 1849-1861 (1966).
- <sup>5</sup>E. Reinhold and W. Ubachs, "Heavy Rydberg states," *Mol. Phys.* **103**, 1329 (2005).
- <sup>6</sup>M. Glass-Maujean, S. Klumpp, L. Werner, A. Ehresmann, and H. Schmoranzler, "Study of the  $B''\bar{B}^1\Sigma_u^+$  state of  $H_2$ : Transition probabilities from the ground state, dissociative widths, and Fano parameters," *J. Chem. Phys.* **126**, 144303 (2007).
- <sup>7</sup>L. Wolniewicz and G. Staszewska, "Excited  $^1\Pi_u$  states and the  $^1\Pi_u \rightarrow X^1\Sigma_g^+$  transition moments of the hydrogen molecule," *J. Mol. Spectrosc.* **220**, 45-51 (2003).
- <sup>8</sup>R. C. Ekey, A. Marks, and E. F. McCormack, "Double resonance spectroscopy of the  $B''\bar{B}^1\Sigma_u^+$  state of  $H_2$ ," *Phys. Rev. A* **73**, 023412 (2006).
- <sup>9</sup>A. de Lange, W. Hogervorst, W. Ubachs, and L. Wolniewicz, "Double-well states of ungerade symmetry in  $H_2$ : First observation and comparison with *ab initio* calculations," *Phys. Rev. Lett.* **86**, 2988-2991 (2001).
- <sup>10</sup>R. C. Ekey, A. E. Cordova, W. Duan, A. M. Chartrand, and E. F. McCormack, "Double resonance spectroscopy of the  $D^1\Pi_u^+$  and  $B''\bar{B}^1\Sigma_u^+$  states near the third dissociation threshold of  $H_2$ ," *J. Phys. B* **46**, 235101 (2013).
- <sup>11</sup>L. Wolniewicz, T. Orlikowski, and G. Staszewska, " $^1\Sigma_u$  and  $^1\Pi_u$  states of the hydrogen molecule: Nonadiabatic couplings and vibrational levels," *J. Mol. Spectrosc.* **238**, 118-126 (2006).
- <sup>12</sup>A. Kirrander and C. Jungen, "Molecular ion-pair states in ungerade  $H_2$ ," *Phys. Rev. A* **84**, 052512 (2011).
- <sup>13</sup>R. C. Ekey and E. F. McCormack, "Spectroscopic observation of bound ungerade ion-pair states in molecular hydrogen," *Phys. Rev. A* **84**, 020501 (2011).
- <sup>14</sup>D. Bailly, E. J. Salumbides, M. Vervloet, and W. Ubachs, "Accurate level energies in the  $EF^1\Sigma_g^+$ ,  $GK^1\Sigma_g^+$ ,  $H^1\Sigma_g^+$ ,  $B^1\Sigma_u^+$ ,  $C^1\Pi_u$ ,  $B'^1\Sigma_u^+$ ,  $D^1\Pi_u$ ,  $I^1\Pi_g$ ,  $J^1\Delta_g$  states of  $H_2$ ," *Mol. Phys.* **108**, 827-846 (2010).
- <sup>15</sup>R. J. Le Roy, LEVEL 8.0: A computer program for solving the radial Schrödinger equation for bound and quasibound levels, University of Waterloo Chemical Physics Research Report CP-663, 2007 see <http://leroy.uwaterloo.ca/programs/>.
- <sup>16</sup>A. Kirrander, private communication (2011).
- <sup>17</sup>S. H. Pan and F. H. Mies, "Rydberg-like properties of rotational-vibrational levels and dissociation continuum associated with alkali-halide charge-transfer states," *J. Chem. Phys.* **89**, 3096-3103 (1988).